

SENSOR AND SIMULATION NOTES

NOTE 197

Cavity Mode Excitation

May 1974

Daniel F. Higgins
C. L. Longmire
Mission Research Corporation

CLEARED
FOR PUBLIC RELEASE

PL/PA 5-12-97

ABSTRACT

In this note a simple prescribed current density is used to analytically calculate the amount of excitation of various cavity modes of a spherical vacuum tank. The source consists of radially moving electrons; both monoenergetic and a more realistic electron energy spectrum are considered. The resultant electric field magnitude of each cavity mode is compared to the static electric field component, with the resulting conclusion that cavity modes are not highly excited by such a current source. (This note was originally prepared as Tank Physics Memo #6, September 1972.)

PL 96-1237

1. INTRODUCTION

In the design of the satellite simulator vacuum tank, a question of interest is the level to which the various electromagnetic modes of the tank will be excited by the burst of photoelectrons made by each X-ray pulse. Since these modes are absent in the case of the satellite in space, we must make sure that they do not seriously degrade the simulation in the tank.

The satellite in space will have several modes of oscillation of its own. For simple structures, the frequency of the lowest mode will be of the order of $c/2d$, where c is the velocity of light and d is the dimension of the structure. These simple modes are damped strongly by radiation. For example, for the lowest mode of oscillation of (the outside of) a conducting sphere, the amplitude decreases by a factor of about 50 per cycle. For complicated structures, there may be modes which have high inductance and capacitance, and which therefore have frequencies which are somewhat lower than $c/2d$. These modes are not so strongly damped by radiation, since their free-space wavelength is somewhat longer than the dimension of the structure.

Because the ejected photoelectrons will mostly have velocities which are small compared with c , the low-frequency satellite modes will tend to be excited most strongly, and they are the modes which are potentially most dangerous for SGEMP. The properties of these modes cannot be guessed without more detailed information on the satellite structure than has been available to us. It will be important to gain

such information at an early date. We wish to point out that simple current injection tests could be used to determine properties of these modes.

When the satellite is placed in the conducting tank, several changes occur. First, the radiation from the satellite modes will be reflected by the walls and reimpinge on the satellite. Degradation of simulation due to this effect can be avoided by reducing the tank wall reflectivity (Q-spoiling) as outlined in Reference 1. Second additional low-frequency modes associated with the tank itself come into play. The frequency of the lowest of these modes is of the order of $c/2D$, where D is the tank diameter. The properties of these modes are not sensitive to the presence or absence of the satellite; as shown in Reference 2, the fractional change in frequency is of the order of the ratio of the satellite volume to the tank volume. These modes can also be damped by reducing the wall reflectivity. However, the low-frequency modes are somewhat harder to damp than those of higher frequency, and are also more strongly excited by slow electrons. Therefore, we have thought it necessary to estimate the level of excitation of the lowest frequency tank mode, in order to assess adequately the damping requirements.

The calculational method used in this memo can be applied to any mode, but is carried through in detail only for the lowest (electric) mode, illustrated in Figure 1, in which the electric field is parallel to the mean direction of electron flow. The satellite is actually ignored except as the source of photoelectrons.

2. THE NORMAL MODE EXPANSION

In the simple model to be considered here, the vacuum tank is treated as a spherical cavity of radius R with perfectly conducting walls. Further assume some current density $\vec{J}(\vec{r}, t)$ within the sphere due to the photoelectrons ejected from the satellite. Also, a high vacuum in the tank gives:

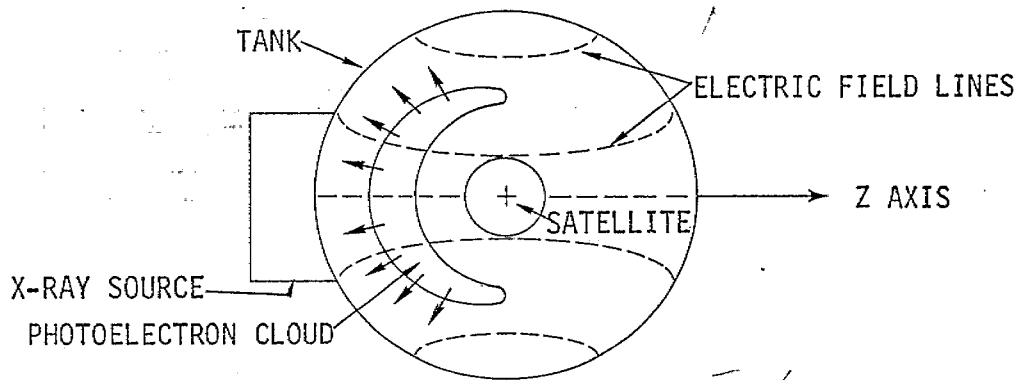


Figure 1. Sketch of configuration assumed.

$$\sigma = 0$$

$$\epsilon = \epsilon_0$$

$$\mu = \mu_0$$

Maxwell's equations are written (MKS units) as

$$\nabla \times \vec{H} = \vec{J} + \epsilon_0 \frac{\partial \vec{E}}{\partial t} \quad (1)$$

$$\nabla \times \vec{E} = -\mu_0 \frac{\partial \vec{H}}{\partial t} \quad (2)$$

Combining these equations one obtains

$$\nabla^2 \vec{H} - \epsilon_0 \mu_0 \frac{\partial^2 \vec{H}}{\partial t^2} = -\nabla \times \vec{J} \quad (3)$$

We now wish to expand the \vec{H} field in terms of the natural modes of the spherical cavity. In general, any \vec{H} can be written as

$$\vec{H} = \frac{i}{Z_0} \sum_n [a_n(t) \vec{m}_n(\vec{r}) + b_n(t) \vec{n}_n(\vec{r})] \quad (4)$$

where \vec{m} and \vec{n} are the vector spherical harmonic functions described in Reference 3, and $Z_0 = 120\pi\Omega$ is the impedance of free space. [As used here the subscript n denotes all the various indices involved in describing the vector spherical harmonic functions.]

Note that each term of the summation is a solution of the sourceless wave equation

$$\nabla^2 \vec{H}_n - \epsilon_0 \mu_0 \frac{\partial^2 \vec{H}_n}{\partial t^2} = 0 \quad (5)$$

This indicates that

$$\nabla^2 \vec{H}_n = -\omega^2 \mu_0 \epsilon_0 \vec{H}_n \quad (6)$$

so that Equation 3 can be rewritten as

$$\omega^2 \vec{H}_n + \frac{\partial^2 \vec{H}_n}{\partial t^2} = \frac{1}{\epsilon_0 \mu_0} (\nabla \times \vec{J})_n \quad (7)$$

where \vec{H}_n is any one term of the series in Equation 4. To find the coefficients $a_n(t)$ and $b_n(t)$ one needs to take the scalar product of \vec{m}_n [or \vec{n}_n] with both sides of Equation 3 and integrate over the volume of the cavity.

To do this one needs to know the orthogonality relationships between the various vector spherical harmonic functions; i.e., one wishes to find the coefficients

$$\alpha_{\vec{e}_{0mn}}(\vec{m}) = \frac{1}{Z_0} \int_0^R \int_0^\pi \int_0^{2\pi} \vec{m}_{0mn} \cdot \vec{m}_{0mn} r^2 \sin\theta dr d\theta d\phi \quad (8)$$

and

$$\alpha_{\vec{e}_{0mn}}(\vec{n}) = \frac{1}{Z_0} \int_0^R \int_0^\pi \int_0^{2\pi} \vec{n}_{0mn} \cdot \vec{n}_{0mn} r^2 \sin\theta dr d\theta d\phi \quad (9)$$

where for the case of interest here, \vec{m} and \vec{n} are written with spherical Bessel functions of the first kind $j_n(r)$ since they have good behavior at $r = 0$. Furthermore, the \vec{m} functions correspond to the electric modes of the cavity where the wave number k is given by the roots of $[kRj(kR)]' = 0$. Also $k = \omega/c$ where c is the velocity of light in a vacuum.

One can evaluate the integrals in Equations 8 and 9 to show that

$$\alpha_{e_{mn}}^{\vec{m}} = \frac{\pi i}{Z_0} (1 + \delta) R^3 \frac{n(n+1)}{2n+1} \frac{(n+m)!}{(n-m)!} \left[1 - \frac{n(n+1)}{\alpha_n^2} \right] j_n^2(\alpha_n) \quad (10)$$

where α_n is a root of $[j_n(\alpha)]' = 0$, and

$$\alpha_{e_{mn}}^{\vec{n}} = \frac{\pi i}{Z_0} (1 + \delta) R^3 \frac{n^2(n+1)}{2n+1} \frac{(n+m)!}{(n-m)!} j_{n+2}(\alpha_n) \quad (11)$$

where α_n is a root of $j_n(\alpha) = 0$. In both Equations 10 and 11

$$\delta = 0 \text{ if } m > 0$$

$$\delta = 1 \text{ if } m = 0.$$

Thus from Equations 3, 4 and 7, one finds

$$\alpha_n^{\vec{m}} [\omega_n^2 a_n(t) + \frac{\partial^2}{\partial t^2} a_n(t)] = \frac{1}{\epsilon_0 \mu_0} \int \vec{m}_n \cdot (\nabla \times \vec{J}) dV \quad (12)$$

where we are considering only the \vec{m} vector coefficients and have used the fact that \vec{m} and \vec{n} are orthogonal. A similar differential equation can be written to find the coefficients $b_n(t)$.

Now let us consider the right hand side of Equation 12. Let

$$\begin{aligned} \Phi &\equiv \frac{1}{\epsilon_0 \mu_0} \int \vec{m}_n \cdot (\nabla \times \vec{J}) dV \\ &= \frac{1}{\epsilon_0 \mu_0} \int_0^{2\pi} \int_0^\pi \int_0^R \vec{m}_n \cdot (\nabla \times \vec{J}) r^2 \sin\theta dr d\theta d\phi \end{aligned} \quad (13)$$

$\nabla \times \vec{J}$ written in spherical coordinates is

$$\begin{aligned}
\nabla \times \vec{J} &= \frac{1}{r \sin \theta} \left[\frac{\partial}{\partial \theta} (\sin \theta J_\phi) - \frac{\partial J_\theta}{\partial \phi} \right] \hat{r} \\
&+ \frac{1}{r} \left[\frac{1}{\sin \theta} \frac{\partial J_r}{\partial \phi} - \frac{\partial}{\partial r} (r J_\phi) \right] \hat{\theta} \\
&+ \frac{1}{r} \left[\frac{\partial}{\partial r} (r J_\theta) - \frac{\partial J_r}{\partial \theta} \right] \hat{\phi}.
\end{aligned} \tag{14}$$

The expression for $\nabla \times \vec{J}$ can be simplified considerably if we pick an appropriate geometry with certain symmetries for the current distribution. To first order, it seems reasonable to assume that \vec{J} has only a radial component and that \vec{J} is ϕ independent; i.e.,

$$\vec{J} = J(r, \theta, t) \hat{r} \tag{15}$$

giving

$$\nabla \times \vec{J} = - \frac{1}{r} \frac{\partial J(r, \theta, t)}{\partial \theta} \hat{\phi} \tag{16}$$

Putting this expression into Equation 13, one obtains

$$\Phi = - \frac{1}{\epsilon_0 \mu_0} \int_0^{2\pi} \int_0^\pi \int_0^R (\vec{m}_n)_\phi \frac{\partial J(r, \theta, t)}{\partial \theta} r \sin \theta dr d\theta d\phi \tag{17}$$

where, from Reference 1

$$(\vec{m}_n)_\phi = - j_n(kr) \frac{\partial P_n^m(\cos \theta)}{\partial \theta} \frac{\cos m\phi}{\sin m\phi}. \tag{18}$$

Note that all terms with $m \neq 0$ will give $\Phi = 0$. Also, if one writes down the ϕ component of the \vec{n} vector, it becomes obvious that the Φ integral with \vec{n} replacing \vec{m} is always zero, since

$$(\vec{n})_\phi = \mp \frac{m}{kr \sin \theta} \frac{\partial}{\partial r} [r j_n(kr)] P_n^m(\cos \theta) \frac{\sin m\phi}{\cos m\phi} \tag{19}$$

Thus the fact that \vec{J} has only a radial component and is axially symmetric (the axis is the same as that of the incident photon beam) leads to the result that \vec{H} can be expanded in terms of the \vec{m} vector spherical harmonics above.

Now consider what simple model can be used to describe the radial current density $J(r, \theta, t)$. The current density is caused by the photoelectrons ejected from the test object when it is hit by the incident photon pulse. For the purposes of calculation assume the satellite is modeled by a small sphere which uniformly ejects photoelectrons over half of its surface (i.e., the illuminated half) where the photon beam enters along the negative z axis. This gives

$$J(r, \theta, t) = J_1(r, t)U(\theta - \frac{\pi}{2}) \quad (20)$$

where $U(\theta)$ is the unit step function. Thus

$$\nabla \times \vec{J} = -\frac{1}{r} J_1(r, t) \delta(\theta - \frac{\pi}{2}) \quad (21)$$

since the δ function, $\delta(\theta - \frac{\pi}{2})$ is the θ derivative of the step function $U(\theta - \frac{\pi}{2})$. Now, Equation 17 can be written as

$$\begin{aligned} \Phi &= \frac{2\pi}{\epsilon_0 \mu_0} \left[\int_0^R j_n(kr) J_1(r, t) r dr \right] \left[\int_0^\pi \frac{\partial P_n(\cos\theta)}{\partial \theta} \delta(\theta - \frac{\pi}{2}) \sin\theta d\theta \right] \\ &= \frac{2\pi}{\epsilon_0 \mu_0} \left[\frac{\partial P_n(\cos\theta)}{\partial \theta} \sin\theta \right] \Big|_{\theta = \frac{\pi}{2}} \int_0^R j_n(kr) J_1(r, t) r dr . \end{aligned} \quad (22)$$

Upon examination of the radial integral, one finds

$$\lim_{r \rightarrow 0} J(r, t) \rightarrow r^\alpha, \quad \alpha \geq -2 \quad (23)$$

if this integral is to be well behaved at the origin.

3. MONOENERGETIC ELECTRONS

Initially, let us consider a δ function distribution of photoelectrons, where all the electrons have the same velocity; then

$$\begin{aligned} J_1(r, t) &= \frac{J_0 \delta(r - vt)}{r^2} \text{ for } 0 \leq t \leq \frac{R}{v} \\ &= 0 \quad \begin{array}{l} t > \frac{R}{v} \\ t < 0 \end{array} \end{aligned} \quad (24)$$

where J_0 is a constant related to the total current. Using this expression for J_1 and letting $n = 1$ for the first modal coefficient, Equation 22 can easily be written as

$$\Phi = - \frac{2\pi k}{\epsilon_0 \mu_0} J_0 \frac{j_1(kvt)}{kvt} , \quad 0 \leq t \leq \frac{R}{v} \quad (25)$$

which, going back to Equation 12, just gives the differential equation

$$\omega_1^2 a_1(t) + \frac{\partial^2}{\partial t^2} a_1(t) = - \frac{2\pi J_0}{\epsilon_0 \mu_0 \alpha_1} \frac{j_1(kvt)}{kvt} . \quad (26)$$

Note that this is just the equation of an oscillator with a time-dependent driving function on the right-hand side. The general solution to this differential equation is the sum of the general solution to the homogeneous equation (i.e., $\sin\omega_1 t$ or $\cos\omega_1 t$ terms) plus a particular solution for the driving function.

Perhaps the simplest method of solving the above equation is by taking the Laplace transform of it; giving

$$a(s) = \frac{\beta}{\omega_1^2 + s^2} \mathcal{L} \left[\frac{j_1(kvt)}{kvt} \right] \quad (27)$$

where

$$\beta = - \frac{2\pi J_0 k}{\epsilon_0 \mu_0 \alpha_1} . \quad (28)$$

Then, from the convolution theorem,

$$a(t) = \frac{\beta}{\omega_1} \int_0^t \sin[\omega_1(t - \tau)] \frac{j_1(kv\tau)}{kv\tau} d\tau . \quad (29)$$

It turns out that the integral in Equation 29 is not easily evaluated analytically. However, over the range of interest (i.e., $0 \leq kv\tau \leq 2.75$) the spherical Bessel function can be approximated quite well by a polynomial in $(kv\tau)$; i.e., write

$$\frac{j_1(kv\tau)}{kv\tau} \approx P(kv\tau) \quad (30)$$

where

$$P(kv\tau) = A + B(kv\tau)^2 + C(kv\tau)^4, \quad \tau < \frac{R}{v} \quad (31)$$

$$= 0, \quad \tau > \frac{R}{v}$$

with

$$A = .33$$

$$B = -.033$$

$$C = 1.19 \times 10^{-3}$$

The function $P(kv\tau)$ is within a few percent of $j_1(kv\tau)/kv\tau$ at the very worst.

Putting this polynomial in Equation 29, one obtains, for $t < \frac{R}{v}$,

$$a(t) \approx \frac{\beta}{\omega_1^2} \left\{ A + B\left(\frac{v}{c}\right)^2 (\omega_1^2 t^2 - 2) + C\left(\frac{v}{c}\right)^4 (\omega_1^4 t^4 - 12\omega_1^2 t^2 + 24) \right\}$$

$$+ \frac{\beta}{\omega_1^2} \left[-A + 2B\left(\frac{v}{c}\right)^2 - 24C\left(\frac{v}{c}\right)^4 \right] \cos\omega_1 t \quad (32)$$

The first term on the right in this equation is the particular solution, or transient, going with the driving function. The second term is the ringing induced by the step rise at $\tau = 0$. For $t > \frac{R}{v}$, a similar equation could be worked out. It would have no transient term, but several oscillating terms, coming from the step rise at $\tau = 0$ and fall at $\tau = \frac{R}{v}$ and from the variation of the driver at times in between. We shall not work out this formula, but shall instead work with just the $\cos\omega_1 t$ term in Equation 32. The reason is that in the next section we shall go to a continuous distribution of electron velocities which will remove the discontinuous step down, and most of the excitation will be due to the step up at $\tau = 0$. (We shall still assume, as we

have here, that the X-ray pulse is a δ function in time, so that all electrons start at the same time.)

Thus we have an expression for the coefficient of the first term in the series

$$\vec{H} = \sum_n \frac{i}{Z_0} a_n(t) \vec{m}_n . \quad (33)$$

We now wish to find the electric field. From Equation 1 we find, using the fact that $\nabla \times \vec{m}_n = k_n \vec{n}_n$,

$$\begin{aligned} \frac{\partial \vec{E}}{\partial t} &= \frac{1}{\epsilon_0} \nabla \times \vec{H} - \frac{\vec{J}}{\epsilon_0} \\ &= \frac{1}{\epsilon_0} \sum_n \frac{i}{Z_0} k_n a_n(t) \vec{n}_n - \frac{\vec{J}}{\epsilon_0} . \end{aligned} \quad (34)$$

Note that

$$\nabla \cdot \vec{m} = \nabla \cdot \vec{n} = 0 \quad (35)$$

but that continuity requires

$$\nabla \cdot \vec{J} = - \frac{\partial \rho}{\partial t} \quad (36)$$

which in this case is not equal to zero. This indicates that \vec{J} must be expanded in terms of the $\vec{\ell}$ vector spherical harmonic in addition to \vec{n} and \vec{m} . The $\vec{\ell}$ vector parts of \vec{J} do not affect \vec{H} , of course, since their curl is zero.

Now, if we take the time integral of both sides of Equation 34, one obtains,

$$\vec{E} = \frac{1}{\epsilon_0} \frac{i}{Z_0} \sum_n k_n \vec{n}_n \int a_n(t) dt - \frac{1}{\epsilon_0} \int \vec{J} dt . \quad (37)$$

Consider only the oscillatory term in the expression of Equation 32 for $a_1(t)$. The integration just changes the $\cos \omega_1 t$ to a $\frac{1}{\omega_1} \sin \omega_1 t$.

Thus the $n = 1$ oscillatory term in the expansion for \vec{E} is just

$$\vec{E}_{osc} \approx \frac{i}{\epsilon_0 Z_0} \frac{\beta}{\omega_1^3} k_1 \left[-A + 2B \left(\frac{v}{c} \right)^2 + 24C \left(\frac{v}{c} \right)^4 \right] \sin \omega_1 t \vec{n}_1 \quad (38)$$

Since this oscillatory field will remain at long times after the X-ray pulse, one needs to compare it to the late-time field seen by a satellite in space. This static field is related to the total charge that has left the satellite, Q , by

$$E_{static} = \frac{Q}{4\pi\epsilon_0 r_1^2} \quad (39)$$

where we have assumed the satellite is a conducting sphere of radius r_1 . This static field is also the end result of the last term in Equation 37.

We now wish to relate this charge Q to the parameter J_0 . By continuity

$$\int_S \vec{J} \cdot \vec{n} dS = - \int_V \frac{\partial \rho}{\partial t} dV \quad (40)$$

which when written in terms of our expression 24 for \vec{J} becomes

$$2\pi J_0 \delta(r - vt) \left[U(0) - U\left(\frac{R}{v}\right) \right] = - \frac{\partial Q}{\partial t} \quad (41)$$

Here we have written the current as a δ function in space times a rectangular pulse in time. Also it is assumed that the satellite was originally uncharged so that the charge that has been ejected is the negative of the charge remaining. Integrating Equation 41 over time, one discovers that

$$J_0 = \frac{Qv}{2\pi} \quad (42)$$

With this expression for J_0 one can go back and directly compare E_{osc} and E_{static} . From Equation 38

$$\begin{aligned} \vec{E}_{osc} &\approx \frac{i}{\epsilon_0 Z_0} \frac{2\pi J_0}{\epsilon_0 \mu_0 \alpha_1} \frac{k_1^2}{\omega_1^3} \left[-A + 2B\left(\frac{v}{c}\right)^2 - 24C\left(\frac{v}{c}\right)^4 \right] \sin\omega_1 t \vec{n}_1 \\ &= \frac{i}{\epsilon_0 Z_0} \frac{c^2 Q v}{\alpha_1} \frac{k_1^2}{\omega_1^3} \left[-A + 2B\left(\frac{v}{c}\right)^2 - 24C\left(\frac{v}{c}\right)^4 \right] \sin\omega_1 t \vec{n}_1 . \end{aligned} \quad (43)$$

For $n = 1$, $kR = 2.75$ and

$$\alpha_1 = (.071) \frac{2\pi i}{Z_0} R^3 \quad (44)$$

which when substituted into Equation 43 gives

$$E_{osc} \approx \frac{Q\left(\frac{v}{c}\right) \left[-A + 2B\left(\frac{v}{c}\right)^2 - 24C\left(\frac{v}{c}\right)^4 \right]}{2\pi\epsilon_0 R^2 (.071) (kR)} \sin\omega_1 t \vec{n}_1 \quad (45)$$

Note that for 30 Kev electrons, $\frac{v}{c} \approx \frac{1}{3}$; thus the higher order $\left(\frac{v}{c}\right)$ terms become very small. Also $|\sin\omega_1 t| \leq 1$ and the maximum value that \vec{n}_1 can have is $2/3$ [this is determined by setting the angular terms in \vec{n}_1 to their maximum value and evaluating at $r = 0$]. Thus, at worst the ratio of oscillatory field to static field is

$$\frac{|\vec{E}_{osc}|}{|\vec{E}_{static}|} \leq 2.26 \left(\frac{r_1}{R}\right)^2 \left(\frac{v}{c}\right) \quad (46)$$

For $r_1 = 4$ meters, $R = 10$ meters and $\frac{v}{c} = \frac{1}{3}$, we find

$$\frac{|\vec{E}_{osc}|}{|\vec{E}_{static}|} \leq .182 . \quad (47)$$

Thus for the simple model used here we find that the maximum electric field due to the lowest tank mode is small compared with the essentially static field due to electrons escaping to infinity (in the case of the satellite in space) or to the tank wall. The "static" field is quite well simulated in the tank experiment, provided its radius is large enough compared with the satellite radius. It therefore

appears that excitation of the tank will only slightly affect the time domain response of the satellite; however, certain bands of the frequency response will be greatly changed.

4. HIGHER ORDER MODES

Now let us consider briefly how much the higher order angular modes are excited. From Equation 22 it can be seen that the angular term gives zero for even values of n due to the particular choice of geometry used here. Thus the next value of n we need to consider is $n = 3$. For $n = 3$,

$$\begin{aligned}\Phi &= \frac{6\pi}{\epsilon_0\mu_0} \int_0^a r j_3(kr) J_1(r, t) dr \\ &= \frac{6\pi J_0}{\epsilon_0\mu_0} \frac{k j_3(kvt)}{kvt}\end{aligned}\quad (48)$$

for the choice of J_1 given in Equation 24.

With this source term, the differential equation we must solve becomes

$$\omega_3^2 a_3(t) + \frac{\partial^2 a_3(t)}{\partial t^2} = \frac{6\pi J_0}{\alpha_3 \epsilon_0 \mu_0} \frac{k j_3(kvt)}{kvt} \quad (49)$$

Now one can expand j_3 in a polynomial as was done for j_1 in Equation 31. Note, however, that the first term in an expansion for $j_3(kvt)$ has a $(kvt)^3$ factor, while the first term of $j_1(kvt)$ was proportional to $(kvt)^1$. Note that this will result in giving an additional $\left(\frac{v}{c}\right)^2$ factor in the solution for $a_3(t)$ [as compared to $a_1(t)$]. This brings down the magnitude of $a_3(t)$ by about 1/9 over that of $a_1(t)$ [ignoring changes in the other coefficients]. Similarly, the $a_n(t)$ term will contain a factor of $\left(\frac{v}{c}\right)^{n-1}$, which indicates that all the higher order modes will be excited much less than the $n = 1$ mode.

Upon evaluating all the coefficients, one obtains

$$\frac{a_3(t)}{a_1(t)} \approx 1.88 \left(\frac{v}{c}\right)^2 = .21 . \quad (50)$$

Thus it can be seen that the higher order terms in the vector spherical harmonic expansion of \vec{E} and \vec{H} will be relatively unimportant, as compared to the lowest order mode.

The discussion above covers the higher angular modes. Let us now consider the higher radial modes. The natural frequencies of these modes are roughly proportional to the mode number; the frequency ω_2 of the second radial mode is about $2.2\omega_1$. It can be seen that the amplitude excited in a given mode is proportional to $1/\omega_n^2$. Therefore the higher radial modes are also relatively unimportant compared with the lowest mode.

5. CONTINUOUS ELECTRON SPECTRUM

Up to this point we have considered only monoenergetic photoelectrons; i.e., all the photoelectrons we assumed to have the same constant velocity, giving a $\delta(r - vt)$ term in the current density. A more realistic case can be treated by calculating the actual velocity spectrum of the ejected photoelectrons. The limiting assumption made here is that the incident photon pulse is very short so that all the photoelectrons are created at the same time. Since we neglect (as previously) the effect of the field on the electrons, the velocity spectrum is time independent.

From Reference 4 the energy spectrum of the incident photon beam can be written as

$$S_x(u) \sim \frac{1}{w_0} \left[\left(\frac{w_0}{u}\right)^{0.3} - \left(\frac{u}{w_0}\right)^{0.7} \right] n_1 n_2 \quad (51)$$

where

$$\eta_1 = \text{foil attenuation} = \frac{1}{T_1} (1 - e^{-T_1}) , \quad T_1 = \left(\frac{u_1}{u}\right)^{2.5} \quad (52)$$

$u_1 = 10 \text{ kev}$

$$\eta_2 = \text{tank window attenuation}$$

$$= e^{-T_2} , \quad T_2 = \left(\frac{u_2}{u}\right)^3 , \quad u_2 = 5 \text{ kev} \quad (53)$$

$w_0 = 100 \text{ kev}$, $u = \text{photon energy in kev}$.

To normalize this expression, let A be the incident energy flux in ergs/cm^2 and

$$I_0 = \int_0^{w_0} S_x(u) du . \quad (54)$$

Thus $\frac{A}{I_0} S_x(u)$ has the dimension of $\frac{\text{ergs}}{\text{cm}^2 \text{kev}}$. The number density spectrum becomes

$$\Phi_x(u) = \frac{1}{1.6 \times 10^{-9} u} \frac{A}{I_0} S_x(u) \frac{\text{photons}}{\text{cm}^2 \text{kev}} \quad (55)$$

For calculations here, we will assume $A = 10^{-5} \text{ cal/cm}^2 = 4.18 \times 10^2 \text{ ergs/cm}^2$. Also, I_0 is calculated numerically to be 0.553.

One can also obtain from References 2 and 3 that the photoelectron yield is given by

$$S_e(w, u) = \frac{3 \times 10^{-2}}{u^3} w \frac{\text{electrons}}{\text{kev photon}} \quad (56)$$

for

$$0 < w < u_{\text{max}} , \quad w = \text{electron energy in kev} .$$

Thus, the spectrum of emitted photoelectrons can be written as

$$\Phi_e(w) = \mathcal{P} \int_w^{w_0} S_e(w, u) \Phi_x(u) du \quad (57)$$

where the units of $\Phi_e(w)$ are electrons/kev and \mathcal{P} is the exposed area

of the target in cm^2 . The functions were evaluated numerically and the resulting energy spectrum is shown in Figure 2.

This energy spectrum can be related to the velocity spectrum, $F(v)$, by the equation

$$\Phi_e(w)dw = F(v)dv . \quad (58)$$

In the classical limit

$$dw = mvdv \quad (59)$$

giving the relation

$$F(v) = mv\Phi_e(w) . \quad (60)$$

Strictly speaking, one should use the relativistic formula relating velocity to kinetic energy. However, the relativistic correction becomes important only for the higher energy electrons, and as seen in Figure 2, there are very few electrons at higher energies compared to the peak. The peak of the energy spectrum is at about 6 keV, which is equivalent to $\frac{v}{c} = .15$. This indicates that classical formulas hold very well at this energy, and thus the above expression for $F(v)$ is fairly accurate.

Using these relations, the velocity distribution shown in Figure 3 is obtained. Now let us consider finding an expression for the radial current density using this velocity distribution. The number of electrons per unit radial interval dr is given by

$$\frac{F(v)dv}{dr} = \frac{F(v)}{t} , (v = r/t) . \quad (61)$$

The current then is just

$$J(r, t) = - e \frac{F(v)}{t} \cdot v \cdot \frac{1}{2\pi r^2} . \quad (62)$$

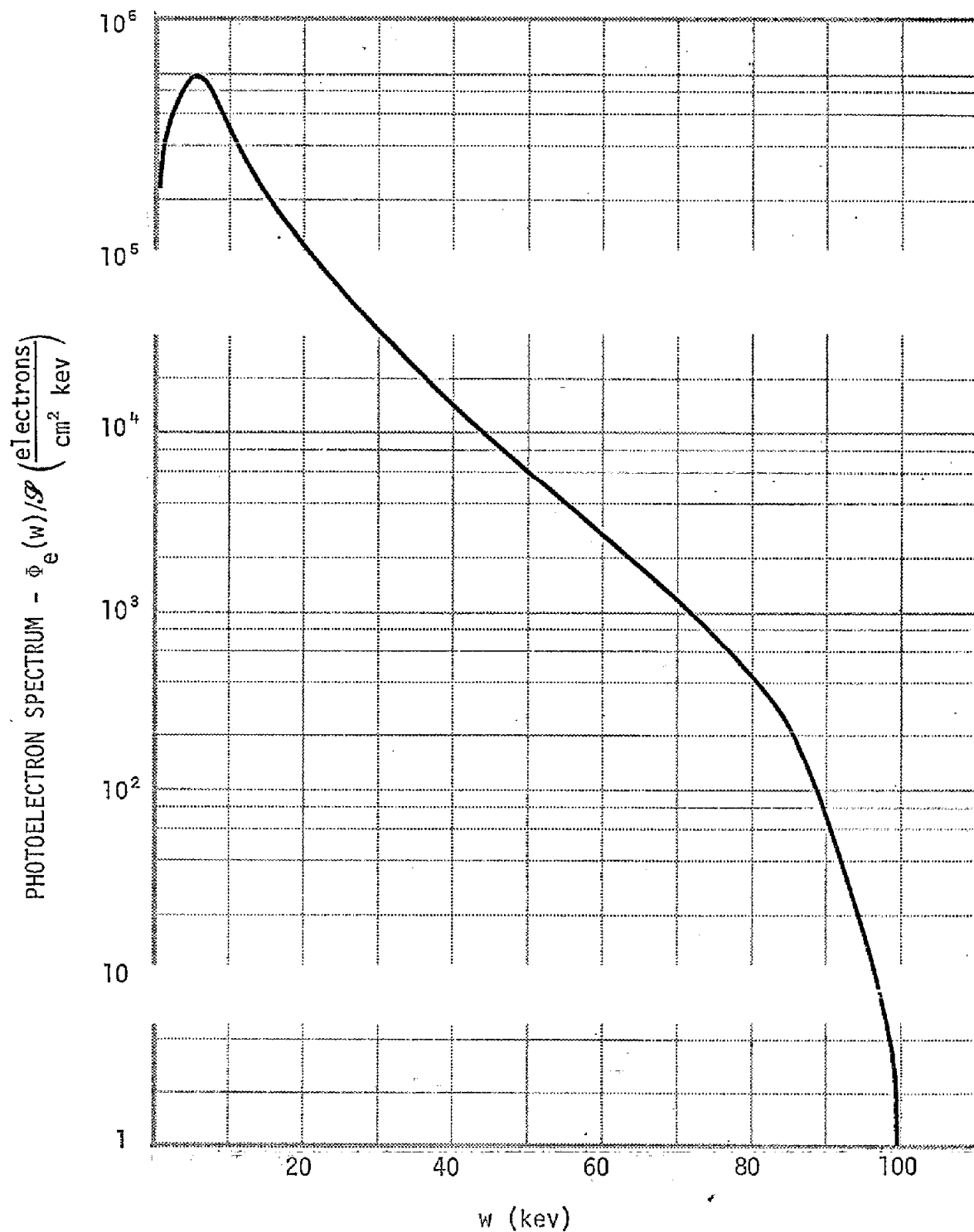


Figure 2. Number of photoelectrons per keV energy per cm² of target area.

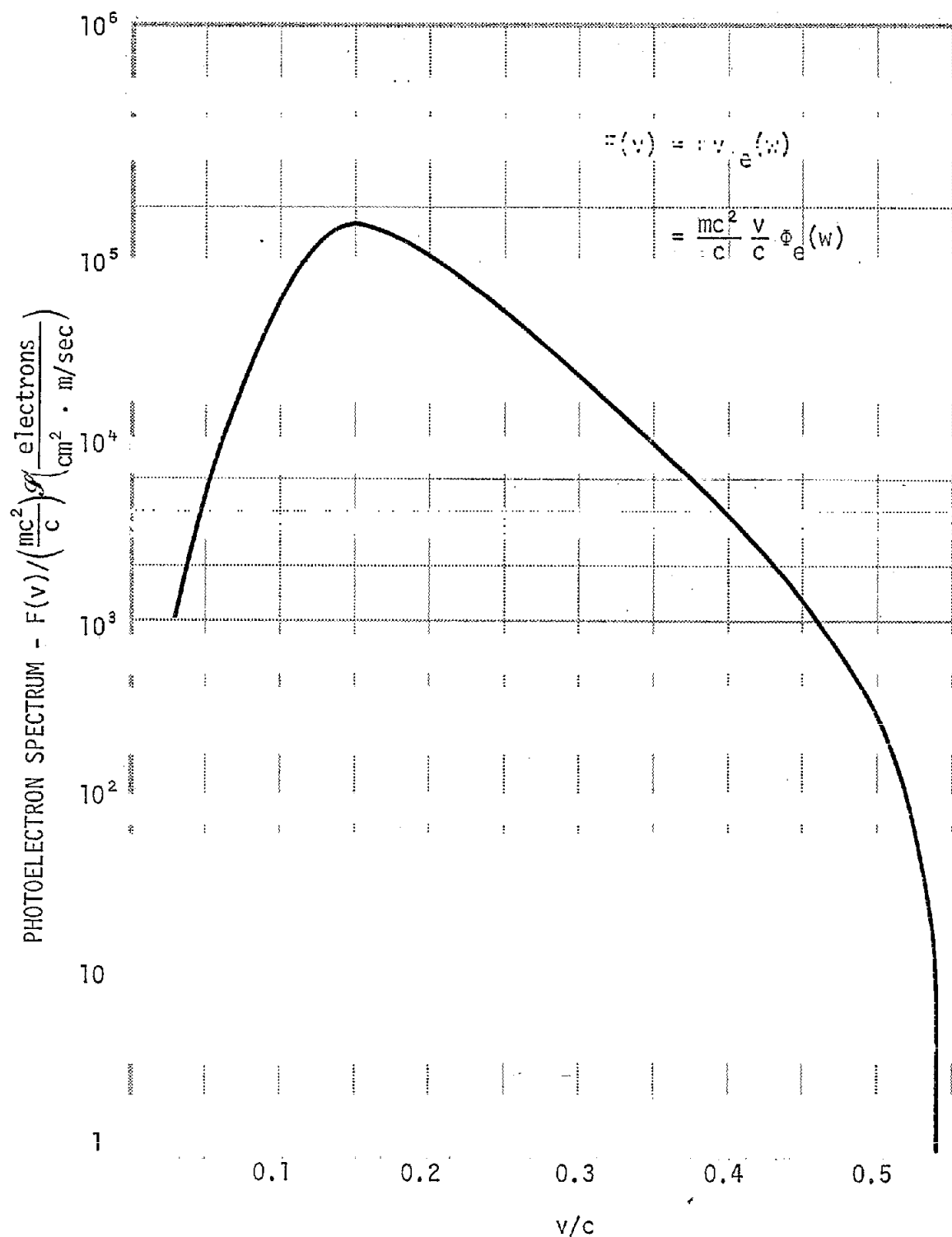


Figure 3. Number of photoelectrons as a function of velocity per cm^2 of target area.

The source term (see Equation 22) in the differential equation for a_1 then becomes

$$\Phi = \frac{2\pi}{\epsilon_0 \mu_0} \int_0^R j_1(kr) \frac{eF(v)}{t} \cdot v \cdot \frac{1}{2\pi r^2} r dr \quad (63)$$

With the substitution $r = vt$, this equation can be written

$$\Phi = \frac{e}{\epsilon_0 \mu_0} \frac{1}{t} \int_0^{\frac{R}{t}} F(v) j_1(kvt) dv \quad (64)$$

Now, approximate $j_1(kvt)$ by the polynomial

$$j_1(kvt) \approx A(kvt) + B(kvt)^3$$

Then

$$\Phi = \frac{e}{\epsilon_0 \mu_0} A \omega \int_0^{v_1/c} \left(\frac{v}{c}\right) F\left(\frac{v}{c}\right) d\left(\frac{v}{c}\right) + \frac{e}{\epsilon_0 \mu_0} B \omega^3 t^2 \int_0^{v_1/c} \left(\frac{v}{c}\right)^3 F\left(\frac{v}{c}\right) d\left(\frac{v}{c}\right) \quad (65)$$

where v_1 is either $\frac{R}{t}$ or v_{\max} , whichever is smaller. [v_{\max} is the velocity of the highest energy photoelectron, which in this case corresponds to $v/c = .549$ (i.e., 100 kev).]

Upon evaluating the integrals

$$I_1 = \int_0^{v_1/c} \left(\frac{v}{c}\right) F\left(\frac{v}{c}\right) d\left(\frac{v}{c}\right) \quad (66)$$

and

$$I_2 = \int_0^{v_1/c} \left(\frac{v}{c}\right)^3 F\left(\frac{v}{c}\right) d\left(\frac{v}{c}\right) \quad (67)$$

one has a time-dependent expression for Φ which is the driving term in the differential equation for $a_1(t)$. Since the time dependence of Φ is a function of the upper limit of I_1 and I_2 , the integration must be carried out for an arbitrary upper limit. Since the integrands of I_1 and I_2 cannot be expressed in terms of simple analytic functions,

the integrals were numerically evaluated for a number of upper limits. The results are shown in Figure 4. Using these graphs one can evaluate Φ as a function of t , for various values of the constants. Φ as a function of time for $R = 10$ meters was calculated and is plotted in Figure 5. It turns out that this curve can be approximated fairly well by the difference of two exponential functions; i.e.,

$$\frac{\epsilon_0 \mu_0}{2\pi \mathcal{P}} \Phi \approx D e^{-\lambda_1 t} - E e^{-\lambda_2 t} \quad (68)$$

where

$$D = 5.9 \times 10^{-6} \quad \lambda_1 = 1.65 \times 10^7 \text{ sec}^{-1}$$

$$E = 4.7 \times 10^{-6} \quad \lambda_2 = 2.39 \times 10^7 \text{ sec}^{-1}$$

Thus the differential equation one must solve for $a_1(t)$ becomes

$$\omega_1^2 a_1(t) + \frac{\partial^2}{\partial t^2} a_1(t) = \frac{2\pi \mathcal{P}}{\alpha_1 \epsilon_0 \mu_0} \left[D e^{-\lambda_1 t} - E e^{-\lambda_2 t} \right]. \quad (69)$$

For a simple exponential driving force the solution of this differential equation is fairly simple. It is found that

$$a_1(t) = \frac{2\pi \mathcal{P}}{\alpha_1 \epsilon_0 \mu_0} \left[\frac{D}{\lambda_1^2 + \omega_1^2} \left(\frac{\lambda_1}{\omega_1} \sin \omega_1 t - \cos \omega_1 t + e^{-\lambda_1 t} \right) - \frac{E}{\lambda_2^2 + \omega_1^2} \left(\frac{\lambda_2}{\omega_1} \sin \omega_1 t - \cos \omega_1 t + e^{-\lambda_2 t} \right) \right]. \quad (70)$$

For the lowest frequency mode, $\omega_1 = 8.25 \times 10^7 \text{ sec}^{-1}$, so that

$$\frac{\lambda_1}{\omega_1} = .20 \quad \text{and} \quad \frac{\lambda_2}{\omega_1} = .29$$

Thus, to a good approximation, $a_1(t)$ can be written as

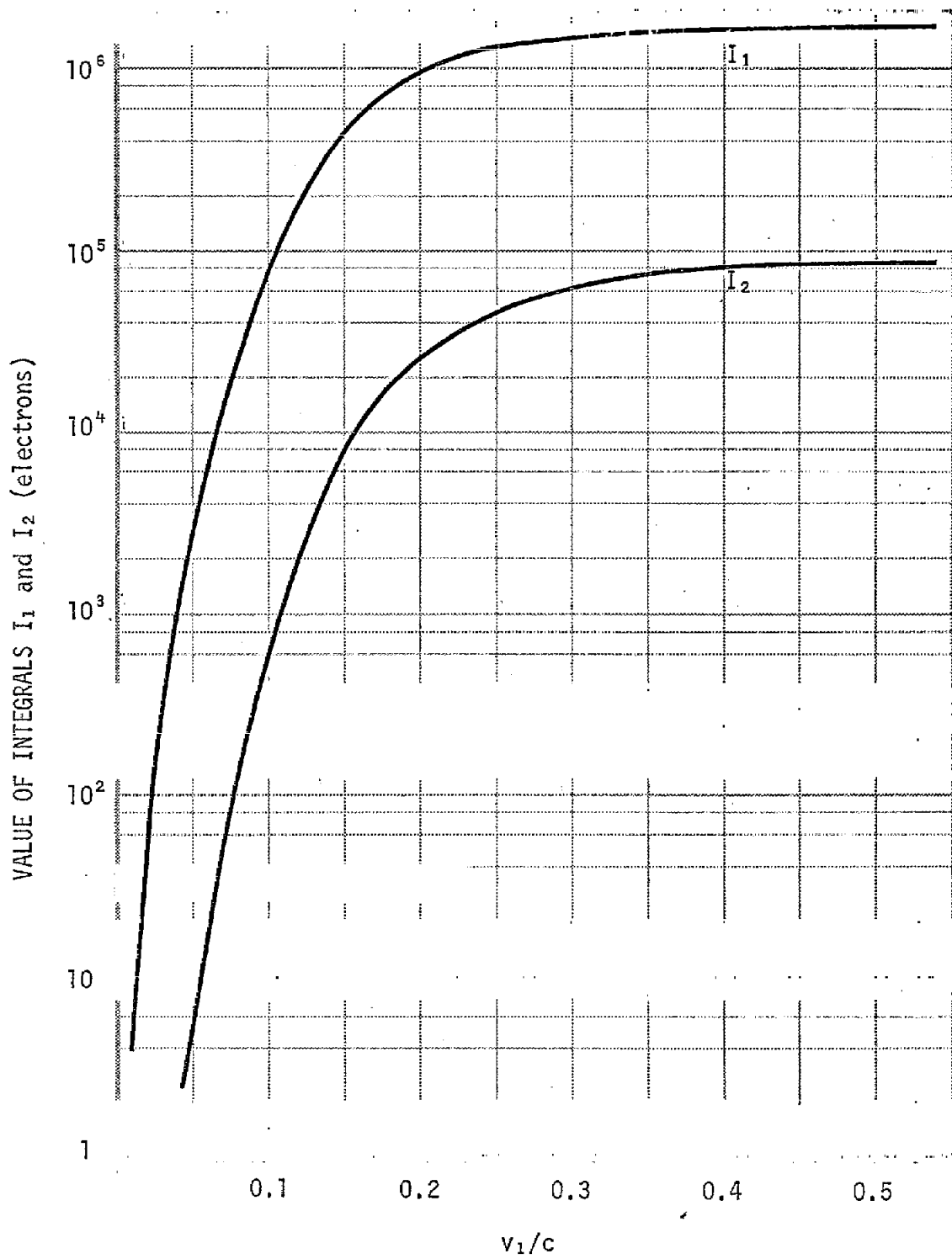


Figure 4. Integrals I₁ and I₂ as a function of $\frac{v_1}{c}$.

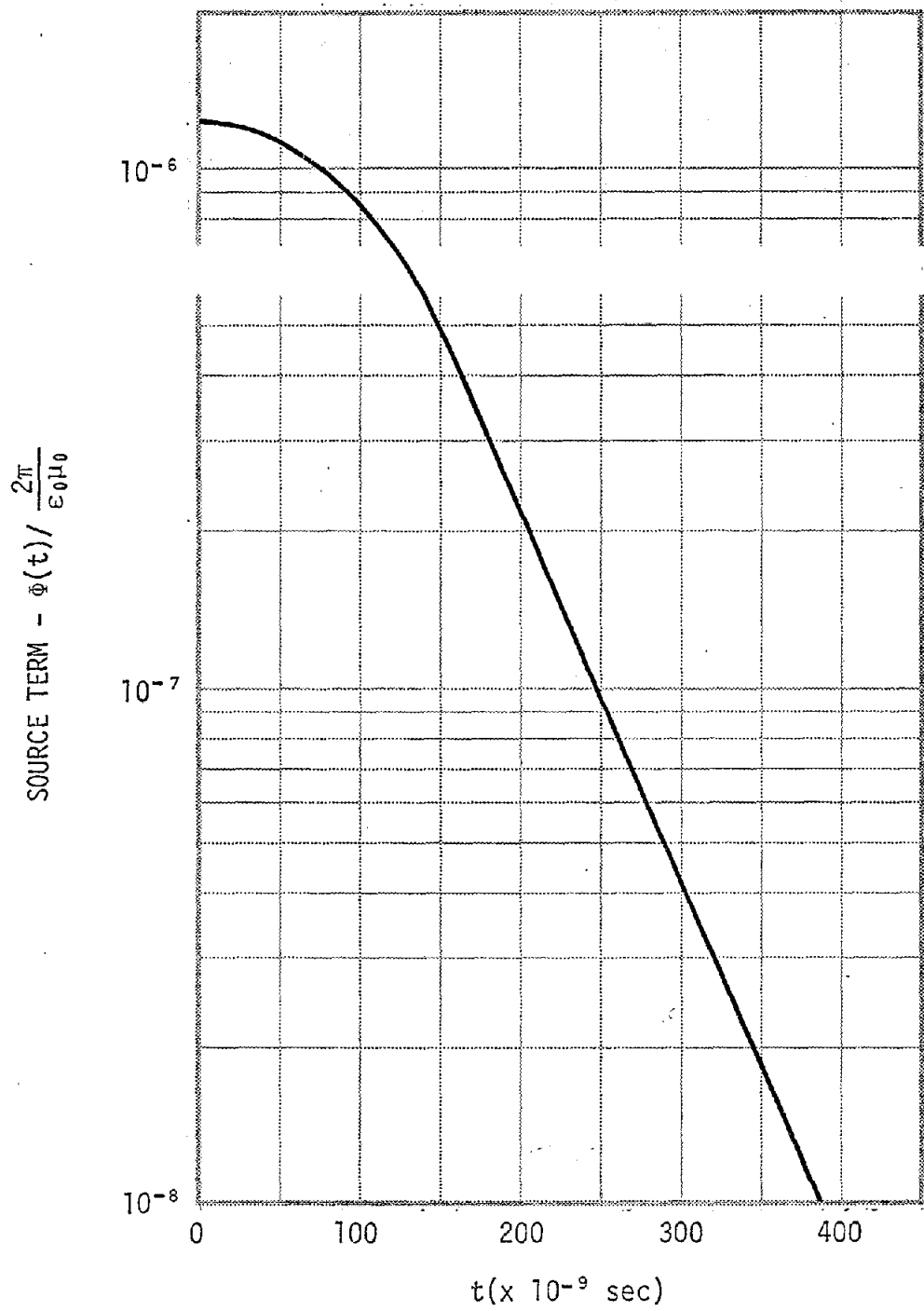


Figure 5. Source term ϕ as a function of time for $R = 10$ meters.

$$a_1(t) \approx \frac{2\mathcal{P}}{\alpha_1 \epsilon_0 \mu_0} \left[\frac{D}{\omega_1^2} \left(-\cos(\omega_1 t + \phi_1) + e^{-\lambda_1 t} \right) - \frac{E}{\omega_1^2} \left(-\cos(\omega_1 t + \phi_2) + e^{-\lambda_2 t} \right) \right] \quad (71)$$

Here ϕ_1 and ϕ_2 are phase angles of the order of $\frac{\lambda_1}{\omega_1}$ and $\frac{\lambda_2}{\omega_1}$. Using this expression to find the oscillatory part of the first mode of the electric field, as was done in Equations 34 to 38, one obtains

$$\vec{E}_{\text{osc}}(n=1) \approx \frac{i}{\epsilon_0 Z_0} \frac{\mathcal{P}}{\epsilon_0} \frac{2\pi c}{\alpha_1} \left[\frac{D}{\omega_1^2} \left(-\sin(\omega_1 t + \phi_1) \right) - \frac{E}{\omega_1^2} \left(-\sin(\omega_1 t + \phi_2) \right) \right] \vec{n}_1 \quad (72)$$

Now, if we set the $\sin(\omega_1 t + \phi)$ and the angular terms in \vec{n}_1 equal to one we have an upper limit on the magnitude of $\vec{E}_{\text{osc}}(n=1)$; namely

$$|\vec{E}_{\text{osc}}(n=1)| \leq \frac{i\mathcal{P}}{\epsilon_0 Z_0} \frac{2\pi c}{\alpha_1} \frac{2}{3} \left[\frac{D-E}{\omega_1^2} \right] \approx \frac{4.99 \times 10^{-10} \text{ coulombs}}{\epsilon_0 \text{ m}^2} \quad (73)$$

We now need to compare this to the static electric field (Equation 39)

$$E_{\text{static}} = \frac{Q}{4\pi\epsilon_0 r_1^2}$$

where Q is the total amount of charge that has left the satellite. Q can be calculated from the energy spectrum of the emitted photoelectrons; i.e.,

$$Q = e \mathcal{P} \int_0^{w_0} \Phi_e(w) dw \quad (74)$$

Evaluating this integral numerically gives $Q = 1.65 \times 10^{-12}$ coulombs per square cm of exposed area. Thus for $r_1 = 4$ meters

$$E_{\text{static}} = \frac{8.25 \times 10^{-9}}{\epsilon_0} \frac{\text{coulombs}}{\text{m}^2} \quad (75)$$

and the ratio

$$\frac{E_{\text{osc}}}{E_{\text{static}}} \approx .060 \quad (76)$$

which is not too different from the ratio obtained for photoelectrons all having the same velocity, obtained in Section 3. The conclusion that excitation of the tank modes does not seriously degrade the simulation is therefore reaffirmed.

6. CONCLUSIONS

We have seen that the oscillating electric fields due to the tank modes are small compared with the essentially static electric field due to electrons escaping from the satellite. This result depended upon the effective radius of the satellite being small compared with the tank radius, and the mean velocity of the photoelectrons being small compared with the velocity of light.

A few comments should be made regarding these results. First, we have compared the cavity mode excited fields to the late-time field seen by the satellite; the question of what happens at intermediate times was not discussed. However, the tank can not affect the early-time response of the satellite since the satellite will not "see" the tank until a signal has had time to travel to the wall and back. We believe the estimate of degradation made above encompasses the problem.

Secondly, one should keep in mind the simplifying assumptions used in these calculations. Azimuthal symmetry about the axis of the

incident photon beam was assumed. A real satellite might be oriented so that this symmetry is not strictly correct. Such an asymmetrical geometry would make mode excitation coefficients more difficult to calculate, but it is hard to imagine a situation which drastically changes the general results obtained here. The same holds true if one considered a more realistic incident photon pulse (i.e., a finite length photon pulse rather than a delta function of time which creates all the photoelectrons at the same instant). We have also assumed that all the ejected photoelectrons have sufficient energy to reach the outer wall. For an incident photon beam with energy density 10^{-5} calories/cm², the satellite will become charged to a potential of a few kev, indicating that most of the ejected electrons will reach the outer wall.

We do have a worry, based on ignorance, concerning the abnormally low-frequency satellite modes. Until we know what these are, we cannot say with certainty that they will not be seriously affected by the presence of the tank, or how much Q spoiling will be needed to decouple them from the tank.

REFERENCES

1. Messier, M. A., and C. L. Longmire, The Damping of Tank Oscillations with Conducting Dielectric Shells, Air Force Weapons Laboratory, Sensor and Simulation Note 196, May 1974.
2. Messier, M. A., The Effect of a Center Conductor on the Resonate Modes of a Spherical Cavity with a Perfectly Conducting Wall, Air Force Weapons Laboratory, Sensor and Simulation Note 195, May 1974.
3. Stratton, J. A., Electromagnetic Theory, McGraw-Hill, 1941. (See sections 7.3-7.14 and 9.22-9.24.).
4. Longmire, C. L., Considerations in SGEMP Simulation, Air Force Weapons Laboratory, Sensor and Simulation Note 194, May 1974.